CHURCHILL LIVINGSTONE

Cell Calcium 33 (2003) 257–266

cell calcium

www.elsevier.com/locate/ceca

Intracellular Ca^{2+} regulates the cellular iron uptake in K562 cells

Weimin Ci [a], Wenyu Li [a], Ya Ke [b], Zhong-Ming Qian [b], Xun Shen [a,*]

[a] *Institute of Biophysics, Chinese Academy of Sciences, 15 Datun Road, Chaoyang District, Beijing 100101, China*

[b] *Department of Applied Biology and Chemical Technology, The Hong Kong Polytechnic University, Kowloon, Hong Kong, China*

Received 27 September 2002; received in revised form 10 November 2002; accepted 11 December 2002

Abstract

Fluorescence quenching was used to study the kinetics of the transferrin receptor (TfR)-mediated iron uptake in the calcein-loaded K562 cells. It was found that elevation of intracellular free Ca^{2+} ($[Ca^{2+}]_i$) by thapsigargin (TG) speeds up the initial rate of iron uptake and increases the overall capacity of the cells in taking up iron. Depletion of intracellular Ca^{2+} or complete chelation of extracellular Ca^{2+} results in complete inhibition of the iron uptake in cells. To gain insight into molecular mechanism, IANBD-labeled transferrin (Tf) and microscopic fluorescence imaging were used to observe the endocytosis and recycling of the Tf–TfR complex in single live cells. The study showed that the preincubation of cells with TG or phorbol myristate acetate (PMA), the direct activator of protein kinase C (PKC), accelerated the endocytosis and recycling of the complex in a dose-dependent manner. W-7, the calmodulin antagonist, and GF109203X, a selected cell-permeant inhibitor of PKC, can reverse the acceleration. Analysis of actin polymerization in controlled, $[Ca^{2+}]_i$-elevated and W-7-treated cells revealed that the actin polymerization is enhanced as $[Ca^{2+}]_i$ is raised, but reduced by W-7. The results suggest that the regulation of actin polymerization by intracellular Ca^{2+} may play a central role in Ca^{2+}-dependent iron uptake.

Keywords: Iron uptake; Transferrin receptor; Intracellular calcium; Endocytosis; Recycling; Actin polymerization

1. Introduction

It has been well established that iron is a "double-edge sword" for human health. It is necessary for cell cycling [1], synthesis of hemoglobin, DNA [2], and some important enzymes [3]. However, iron overload in the human body can cause cell death and tissue damage through iron-catalyzed Fenton chemistry [4]. Abnormally high levels of iron in the brain have been demonstrated in a number of neurodegenerative disorders, including Hallervorden-Spatz Syndrome, Parkinson's disease, and Alzheimer's disease [5–8]. Therefore, how cells regulate their iron uptake and how to intervene in the regulation of the iron uptake in cells have become interesting subjects for health study. Although several transferrin (Tf)-independent ways of cellular iron uptake have been identified [9], in general, the transferrin receptor (TfR)-mediated pathway is still considered as the main route in cellular uptake of iron. Several steps are involved in the TfR-mediated iron uptake [10]. They are (1) binding of Tf to the TfR on cell membrane; (2) internalization of the complex of iron-bound Tf and its receptor; (3) acidification of endosome by H^+-ATPase; (4) dissociation and reduction of iron ions; (5) translocation of iron across membrane of endosomes by a carrier or channel; (6) iron binding to low-molecular weight cytosolic molecules, such as ATP or AMP, followed by entrance into a particular location for usage, such as the synthesis of heme and other iron-containing proteins, such as ferritin; and (7) return of the Tf–TfR complex to the membrane. Previous studies on the regulation of the TfR-mediated iron uptake have been mainly focused on the TfR expression, its recycling, and the regulatory role of some protein kinases [11–13]. However, no systematic investigation on the role of intracellular free calcium in the TfR-mediated cellular iron uptake and the regulation of either the TfR expression or the recycling of Tf–TfR complex has been reported, though the intracellular Ca^{2+}

Abbreviations: BAPTA, 1,2-bis(2-aminophenoxy)ethane-*N*,*N*,*N*′,*N*′-tetraacetic acid; EGTA, ethylene glycol-bis(β-aminoethyl ether)-*N*,*N*,*N*′,*N*′-tetraacetic acid; IANBD, *N*,*N*′-dimethyl-*N*-(iodoacetyl)-*N*′-(7-nitrobenz-2-oxa-1,3-diazol-4-yl); W-7, *N*-(6-aminohexyl)-5-chloro-1-naphthalenesulfonamide; NTA, nitrilotriacetic acid; Tf, transferrin; TfR, transferrin receptor; PMA, phorbol myristate acetate; PKC, protein kinase C; TG, thapsigargin; LPC, lysopalmitoylphosphatidylcholine

* Corresponding author. Tel.: +86-10-64888574; fax: +86-10-64871293.

E-mail address: shenxun@sun5.ibp.ac.cn (X. Shen).

0143-4160/03/$ – see front matter © 2003 Elsevier Science Ltd. All rights reserved.
doi:10.1016/S0143-4160(02)00240-3

is considered as an important second messenger in a wide variety of signaling pathways. Perhaps the most systematical study on the regulation of TfR recycling by intracellular Ca^{2+} was reported by Sainte-Marie et al. [14]. The results of their study suggest that the intracellular Ca^{2+} concentration plays an important role in the outward flow of TfRs. However, either connection of their results to the actual TfR-mediated cellular iron uptake or the molecular mechanisms involved in the regulation was not given. In this study the kinetics of the TfR-mediated iron uptake in the cells with different concentration of intracellular Ca^{2+} were directly observed. The numbers of TfR expressed on cell surface and the recycling kinetics of Tf–TfR complex, including both internalization and the outward flow, were measured. The possible mechanisms involved in the regulation of the recycling of the Tf–TfR complex by intracellular Ca^{2+} were also explored.

Since iron ions traffic between different cellular stations in the cell, such as Tf-containing endosomes, cytosolic ferritin, or other target stations in cytosol and organelles [15], and the crossroad between the different stations has been associated with a cytoplasmic pool of low-molecular weight molecule-complexed iron [15,16], which is also presumed to be the intermediated intracellular target of iron chelators [17], the transient change in such a chelatable iron pool initiated by the binding of Tf to TfR may be an even better measure for observing the TfR-mediated iron uptake by cells. Such observation not only provides kinetic information on cellular uptake of iron, but also offers a good approach to study the signal transduction in TfR-mediated iron uptake. Here, we studied the process of the iron uptake initiated by the binding of Tf to its receptor via direct observation of the transient change in the cytoplasmic chelatable pool in K562 cells loaded with the fluorescence probe, calcein, as an iron chelator whose fluorescence can be quenched by the iron ions entered into the pool [18]. Thapsigargin (TG), a potent endomembrane Ca^{2+}-ATPase inhibitor which can release Ca^{2+} from intracellular store and induce a maintained elevation of intracellular Ca^{2+} by store depletion-operated Ca^{2+}-influx with minimal disturbances of other signaling mechanism [19,20], was used to establish various intracellular calcium concentration in the cells and to see its regulation on iron uptake, number of TfRs on cell surface and endocytosis of the Tf–TfR complex as well as the actin polymerization.

2. Materials and methods

2.1. Chemicals

Calcein acetoxymethyl ester (calcein-AM), fura-2, Tf (from human serum), *N*-((2-(iodoacetoxy)ethyl)-*N*-methyl) amino-7-nitrobenz-2-oxa-1,3-diazole (IANBD ester), BODIPY FL conjugate, BODIPY FL phallacidin, and 1,2-bis (2-aminophenoxy)ethane-*N*,*N*,*N*′,*N*′-tetraacetic acid acetoxymethyl ester (BAPTA-AM), were purchased from Molecular Probes. Human apo-transferrin, ferric ammonium citrate, nitrilotriacetic acid (NTA), TG, *N*-(6-aminohexyl)-5-chloro-1-naphthalenesulfonamide (W-7), GF109203X, phorbol myristate acetate (PMA), lysopalmitoylphosphatidylcholine (LPC), and ethylene glycol-bis(β-aminoethyl ether)-*N*,*N*,*N*′,*N*′-tetraacetic acid (EGTA) were from Sigma.

2.2. Preparation of iron-saturated Tf

Ferric ammonium citrate (3.24 mg) and NTA (5.37 mg) were dissolved in 10 ml 0.5 M Tris–HCl buffer containing 0.1 mM $NaHCO_3$ (pH 8.5). Ten milligrams of apo-transferrin was added in the solution, and then kept for at least 1 h to allow sufficient complexation of Fe^{3+} with Tf. The iron-saturated Tf was separated from non-bonded Fe^{3+} by three times dialysis in 500 ml HBS buffer (150 mM NaCl, 2 mM $CaCl_2$, 10 mM HEPES–Tris, pH 7.3), and each dialysis took 3 h.

2.3. Labeling of Tf with IANBD

Referring to the method described by Shore et al. [21], the iron-saturated Tf was labeled with fluorescence probe, IANBD ester, with minor modification. The IANBD-labeled Tf was checked fluorometrically, and found its maximal excitation at 478 nm and maximal emission at 540 nm.

2.4. Cell preparation and loading with calcein

Human erythroleukemia K562 cells were grown at 37 °C in DMEM medium containing 10% fetal bovine serum. Cells were loaded with 0.125 μM calcein-AM according to the literature [18]. Excess calcein-AM on cell surface was removed by three washes with Hank's balanced salt solution (HBSS, pH 7.4), the cells were resuspended in DMEM–HEPES medium at the density of 2×10^6 cells/ml and maintained at 37 °C for a minimum of 4 h to deplete intracellular store of Tf. Then the calcein-loaded cells were washed twice, resuspended in 2 ml of prewarmed HBS buffer, and transferred to a quartz cuvette for fluorescence assay on iron uptake in a fluorescence spectrophotometer.

2.5. Fluorescence measurement of iron uptake in suspended cells

Calcein fluorescence (excitation, 488 nm; emission, 517 nm; slits, 10 nm) of above mentioned calcein-AM-loaded cells (in cuvette containing 2×10^6 cells/ml and 2 ml HBS buffer) was measured in a Hitachi F-4500 fluorescence spectrophotometer equipped with a temperature-controlled cuvette holder and magnetic stirrer. During the 25-min measurement, the first 5 min was taken as baseline, then 50 μg/ml iron-bound Tf was added.

2.6. Measurement of free cytosolic Ca^{2+} using fura-2

K562 cells (1×10^6 cells/ml) were loaded with fura-2 by incubation with 1 μM fura-2/AM at 37 °C for 40 min. Cells were then washed twice and resuspended in HBS buffer. The loaded cells (2×10^6 cells/ml, 2 ml) were transferred into magnetic stirring cuvette and measured at 37 °C on a dual excitation fluorescence spectrophotometer (Hitachi F-4500). The fluorescence of the cytosolic Ca^{2+}-bound fura-2 excited at 340 and 380 nm, F_{340} and F_{380}, were recorded simultaneously at the emission of 510 nm. $[Ca^{2+}]_i$ was calculated according to Tsien et al. [22].

2.7. Measurement of the expressed TfRs on cell surface

The number of the TfRs on cell surface was measured as the fluorescence from the BODIPY FL dye-labeled iron-saturated Tf bound to the receptor by flow cytometry. In brief, the cells (10^6/ml, 0.5 ml), which were either treated with TG for 10 min or untreated, were incubated with Tf–BODIPY FL conjugate (30 μg/ml) on ice for about 1.5 h. Then, after three times wash with PBS buffer, 10^4 cells/sample were analyzed on a Coulter Epics flow cytometer (excitation, 488 nm; emission, 540 nm).

2.8. Imaging of the uptake and the recycling of IANBD-labeled Tf

One milliliter of cell suspension (5×10^5 cells/ml in HBSS buffer) was transferred to the glass-bottomed dish and incubated for 15 min at 37 °C. The fluorescence (excitation, 478 nm; emission, >520 nm) of the attached single cells on the bottom glass before and after addition of 50 μl IANBD-labeled Tf (20 μg/ml) into the central field was monitored under Nikon Diaphot 300 inverted microscope equipped with AquaCosmos Microscopic Image Acquisition and Analysis System provided by Hamamatsu Photonics K.K. (Japan). The digitized fluorescence images of the IANBD-labeled Tf in cells and the kinetic change of the fluorescence in single cells were obtained and processed on line on a PC.

2.9. Measurement of F-actin content

The flow cytometric measurement of F-actin was referred to literature [23]. In brief, after incubation with TG for 7 min or W-7 for first 8 min and then together with TG for another 7 min at 37 °C, the cells (10^6/ml, 1 ml) were fixed with 3.7% formaldehyde in ice bath for 15 min. The cells were then permeabilized with LPC (50 μg/ml) to increase the membrane permeability and simultaneously stained with 1.5 units of BODIPY FL phallacidin for 30 min at room temperature. Cells (10^4/sample) were analyzed on the same Coulter Epics flow cytometer.

3. Results

3.1. The iron uptake induced fluorescence quenching in cells and the regulation of iron uptake by intracellular free Ca^{2+} ($[Ca^{2+}]_I$)

As shown in Fig. 1B, upon the addition of iron-saturated Tf (50 μg/ml) in the cell suspension, fluorescence of the calcein-loaded cells begins to decrease without detectable time lag. The fluorescence declines at a gradually reduced rate and finally reaches a lower steady level. The whole fluorescence quenching process takes place for about 20 min,

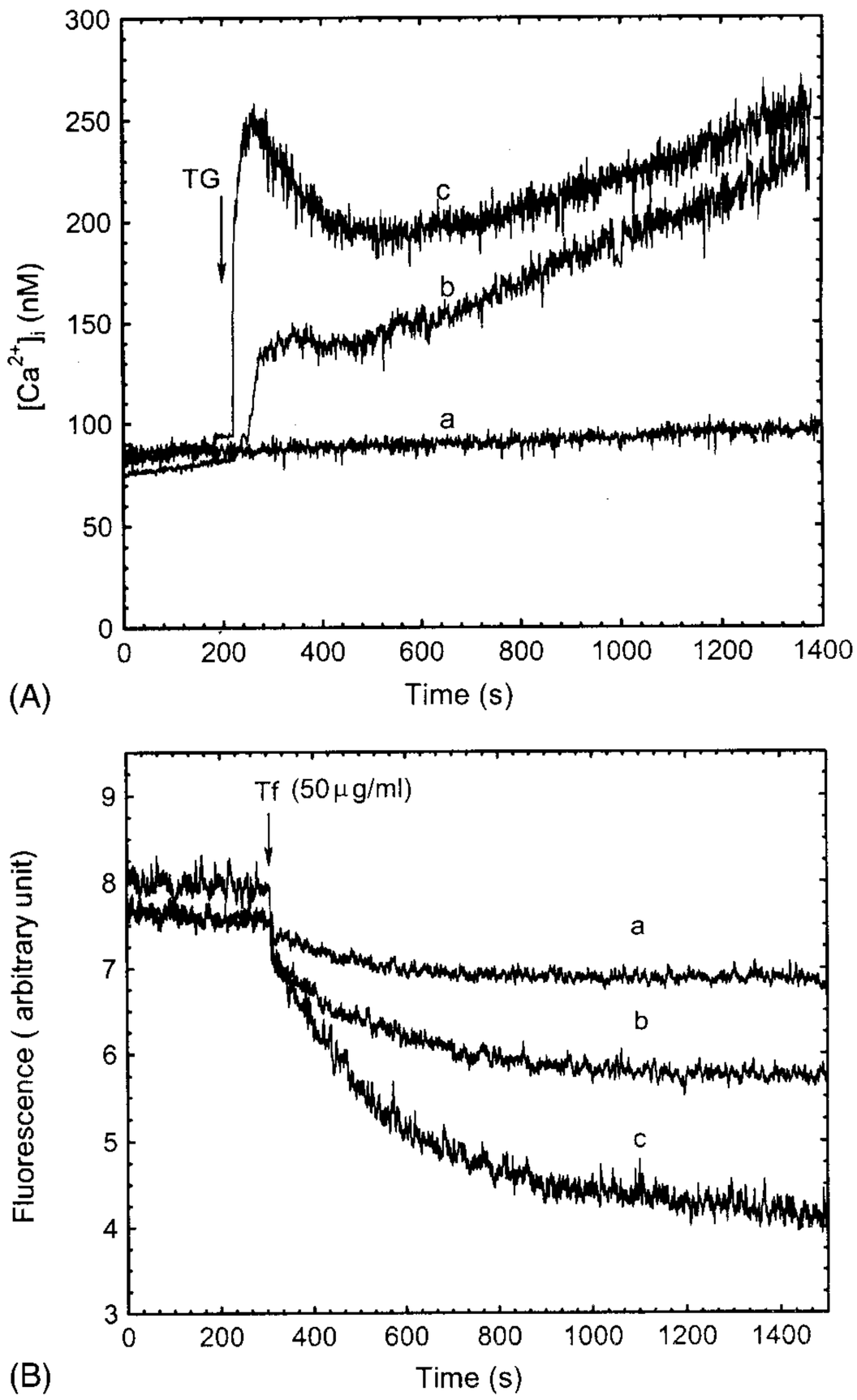

Fig. 1. Elevation of intracellular free Ca^{2+} by thapsigargin and the fluorescence quenching by transferrin-bound iron in the fluorescencein calcein-loaded K562 cells. (A) The cells were loaded with fura-2/AM, and the intracellular Ca^{2+} concentration was measured at 37 °C before and after addition of 0 (a), 2 (b), and 5 nM (c) thapsigargin in cell suspension, respectively, on a dual excitation fluorescence spectrophotometer. (B) Iron-saturated transferrin (50 μg/ml) was added in 2 ml calcein-loaded cell suspension (2×10^6/ml, in HBS buffer, pH 7.3) preincubated with 0 (a), 2 (b), and 5 nM (c) thapsigargin for 10 min, respectively. The fluorescence from the calcein-loaded cell suspension in a magnet stirring cuvette was time scanned at 37 °C on a fluorescence spectrometer.

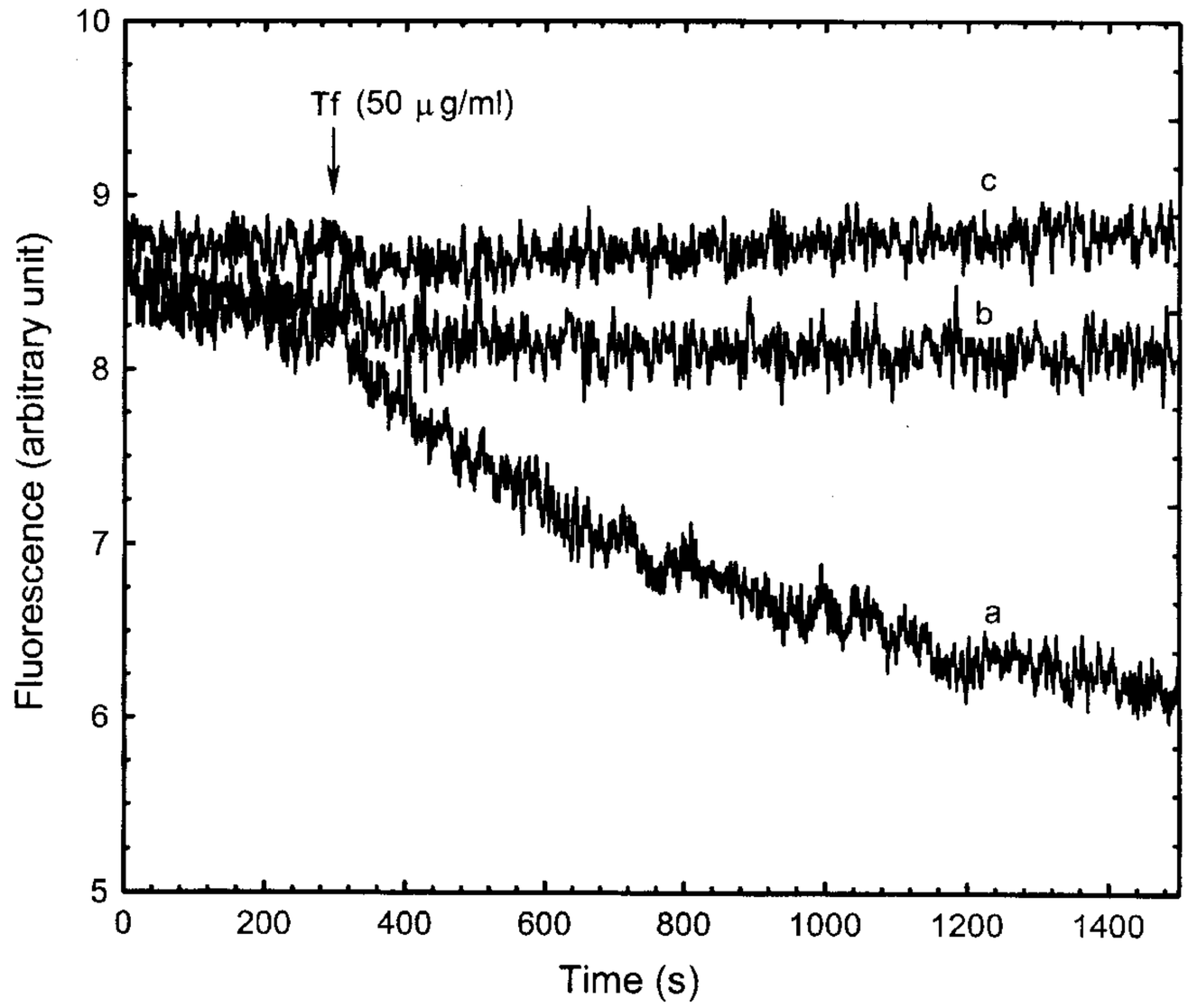

Fig. 2. Quenching of the fluorescence from the calcein-loaded K562 cells (2×10^6 cells suspended in 2 ml HBS solution) induced by the iron-saturated transferrin (50 μg/ml) when intracellular Ca^{2+} or extracellular Ca^{2+} is depleted. The quenching kinetics in controlled cells (curve a) and the cells preincubated with 2.5 μM BAPTA-AM (curve b) or 3 mM EGTA (curve c) for 10 min was measured at 37 °C in a magnet stirring cuvette on a fluorescence spectrometer.

which means that a flashed Tf-bound iron enters into cytoplasmic pool in cells within this time scale.

The kinetic processes of iron uptake were measured in the cells preincubated with TG of various concentrations for 10 min. As shown in Fig. 1A, the intracellular calcium concentration, $[Ca^{2+}]_i$, was elevated from 85 nM to above 150 and 200 nM in the cells treated with 2 and 5 nM TG, respectively. The quenching kinetics of the fluorescence from the TG-treated cells is similar to that from the controlled cells. It clearly demonstrates that both the rate, at which

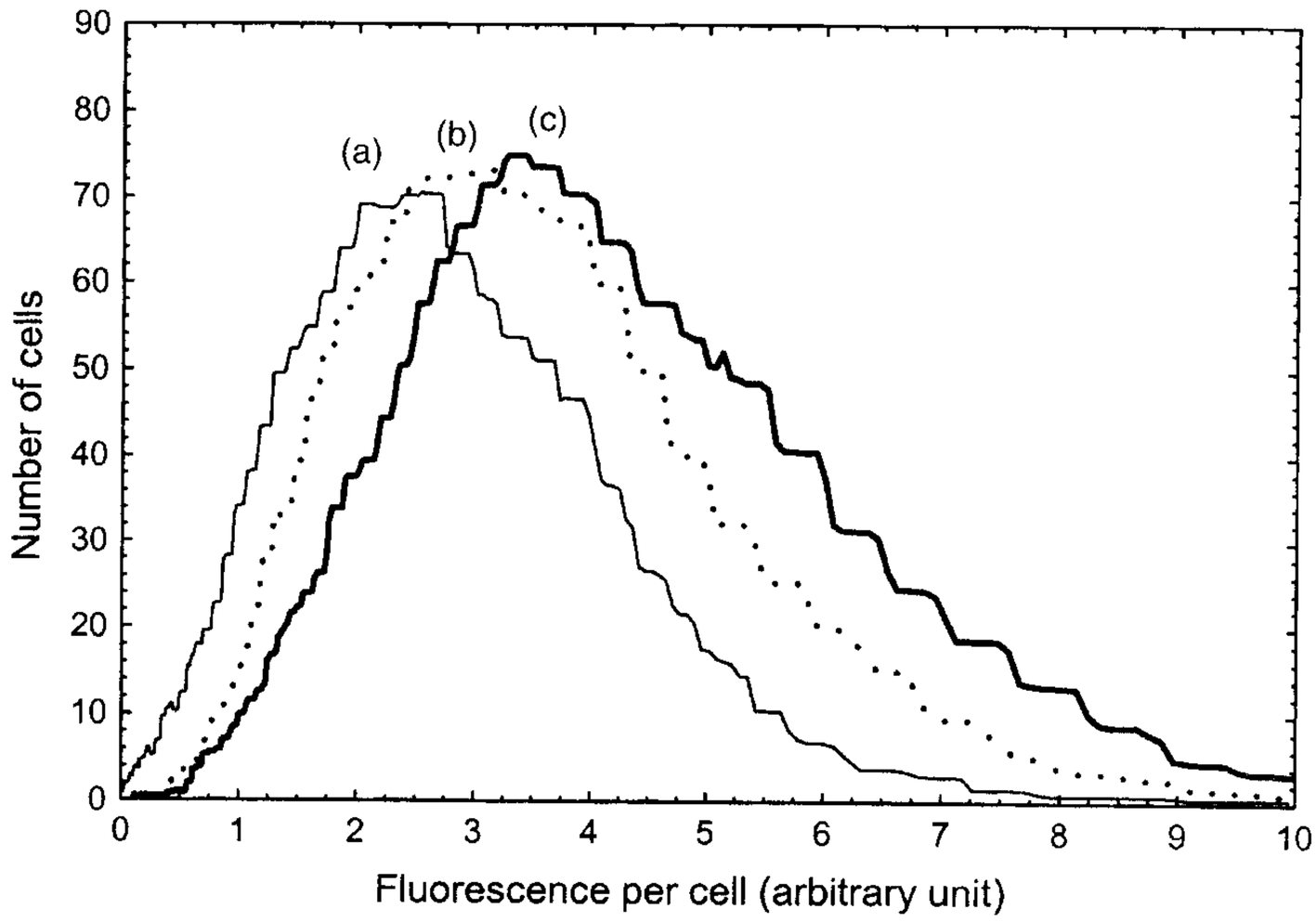

Fig. 3. Regulation of the transferrin receptors expressed on cell surface by intracellular Ca^{2+}. The intracellular Ca^{2+} was elevated by incubation of cells with thapsigargin for 10 min before fluorescence-labeled transferrin was added (see "Section 2"). The distribution of cell numbers against the fluorescence of the BODIPY FL dye-labeled Tf bound to the TfRs per cell was obtained by analysis of 10^4 K562 cells with a flow cytometer. The controlled cells (curve a), the cells treated with 2 nM thapsigargin (curve b) and 5 nM thapsigargin (curve c) were analyzed, respectively. The curves shown here are representatives of three independent measurements.

the uptaken iron quenched the fluorescence, and the finally quenched fluorescence, which represents the total amount of the iron entered into cytosolic pool, increased by the TG treatment in a dose-dependent manner. In particular, the initial rate of iron uptake by cells significantly increased with increasing concentration of TG. The elevation of $[Ca^{2+}]_i$ by 2 and 5 nM TG resulted in 2.5- and 6-fold increases in the overall iron uptake, or 1.7- and 3.8-fold increases of the initial uptake rate, respectively. In order to further examine the role of $[Ca^{2+}]_i$ in the cellular uptake of iron, the effect of BAPTA-AM, the permeable chelator for intracellular Ca^{2+}, and EGTA, the extracellular Ca^{2+} chelator, on the iron uptake in suspended cells were investigated. As shown in Fig. 2, either BAPTA-AM or EGTA almost completely inhibited the iron uptake by cells. Both the observed increase of the iron uptake rate in the TG-treated cells and the suppression of the iron uptake by depleting intracellular or extracellular free Ca^{2+} clearly demonstrate the role played by $[Ca^{2+}]_i$ in regulating the TfR-mediated iron uptake.

3.2. Effect of intracellular Ca^{2+} on the TfRs expressed on cell surface

To know how the elevated intracellular Ca^{2+} upregulates the iron uptake, the expressed TfRs on cell surface were determined in the cells with different intracellular steady-state calcium levels. As described in "Section 2", the numbers of the TfR bound to the fluorescence-labeled Tf were analyzed using flow cytometry. The analysis showed that the cell number distributions against fluorescence intensity per cell, which represents the numbers of the occupied TfR on cell surface, in TG-treated cells were slightly shifted to right (i.e. to higher value of the mean fluorescence per cell). Fig. 3 shows the typical results of three independent analyses.

3.3. Accelerated recycling of the Tf–TfR complex in TG-treated cells and the reverse effect of W-7 or GF109203X

To explore if recycling rate of the Tf–TfR complex is regulated by intracellular Ca^{2+}, the fluorescence probe, IANBD ester, was used to label Tf. As described in "Section 2", 50 μl concentrated IANBD-labeled Tf was added in central field of the glass-bottomed dishes and the fluorescence from the attached cells were pulse-chased under a digital fluorescence microscope. The fluorescence microscopic images of either controlled cells or the cells preincubated with TG were taken every 20 s before and after addition of the fluorescence-labeled Tf. A typical set of the fluorescence images of cells during a single-round endocytosis and recycling of the IANBD-labeled Tf–TfR complex and the kinetic change of the IANBD fluorescence in six randomly selected cells are shown in Fig. 4. The images clearly show that the fluorescence of cells starts rise upon addition of the IANBD–Tf, reaches to its maximum at about 18 min, then declines to a lower steady level at about 38 min. The rising phase represents the endocytosis, and the decline phase may reflect the exocytosis of the Tf–TfR complex after releasing Tf-associated iron into cytosol. In addition to the observation of controlled cells and the cells preincubated with 5 nM TG, the endocytosis and recycling of the IABND–Tf–TfR complex was also observed in the cells preincubated either with W-7, a widely used calmodulin antagonist [24–26] or GF109203X, a selected cell-permeant inhibitor of protein kinase C (PKC) [27,28], for first 5 or 25 min, respectively, and then with TG for an additional 5 min. The fluorescence intensities in the selected cells were followed kinetically in each case. A typical set of results of three randomly selected cells from one of five independent observations is shown in Fig. 5. It was interesting to notice that the cells treated with 5 nM TG transcytosed the Tf–TfR complex more rapidly than the controlled cells (see Fig. 5A and B). The results show that it took about 18 and 12 min to complete the endocytosis of the Tf–TfR complex, but about 35 and 25 min to complete the whole transcytosis of the complex in the controlled and 5 nM TG-treated cells, respectively. However, when 1 μM GF109203X was present in the cell suspension, the acceleration of the Tf–TfR complex recycling by TG was no longer observed, and the time needed for completing the whole cycle became even slightly longer than that observed in the cells without TG treatment (see Fig. 5C). It was also found that the presence of 50 μM W-7 in the cell suspension reversed the TG effect. The Tf–TfR recycling in the cells preincubated with W-7 plus TG became significantly slower than that observed in the cells preincubated only with TG (see Fig. 5D). The results shown in Fig. 5 clearly demonstrate that the recycling of the Tf–TfR complex is accelerated in $[Ca^{2+}]_i$-elevated cells. However, either the inhibitor of PKC or the calmodulin antagonist can reverse this effect.

3.4. PKC involvement in regulation of the Tf–TfR recycling

Since the PKC inhibitor, GF109203X, could reverse the acceleration of the Tf–TfR recycling in TG-treated cells (shown as Fig. 5C), it was natural to investigate the role of PKC in regulating the recycling of the complex in cells. The endocytosis and recycling of the IANBD-labeled Tf–TfR complex in the controlled cells and the cells preincubated with 10 or 100 nM PMA, a widely used direct activator of PKC, for 10 min was observed under a fluorescence microscope. Same as the procedure in observing the complex recycling in the TG-treated cells, the fluorescence intensities in the selected cells were followed kinetically before and after addition of the pulsed IANBD–Tf in each case. A typical set of results of three randomly selected cells from one of five independent observations is shown in Fig. 6. Fig. 6A shows the recycling of the IANBD–Tf–TfR complex in controlled cells. When cells were treated with 10 and 100 nM PMA, respectively, the recycling of the Tf–TfR complex was accelerated in a dose-dependent manner as shown in Fig. 6B and C, respectively. Fig. 6D shows that the endocytosis and

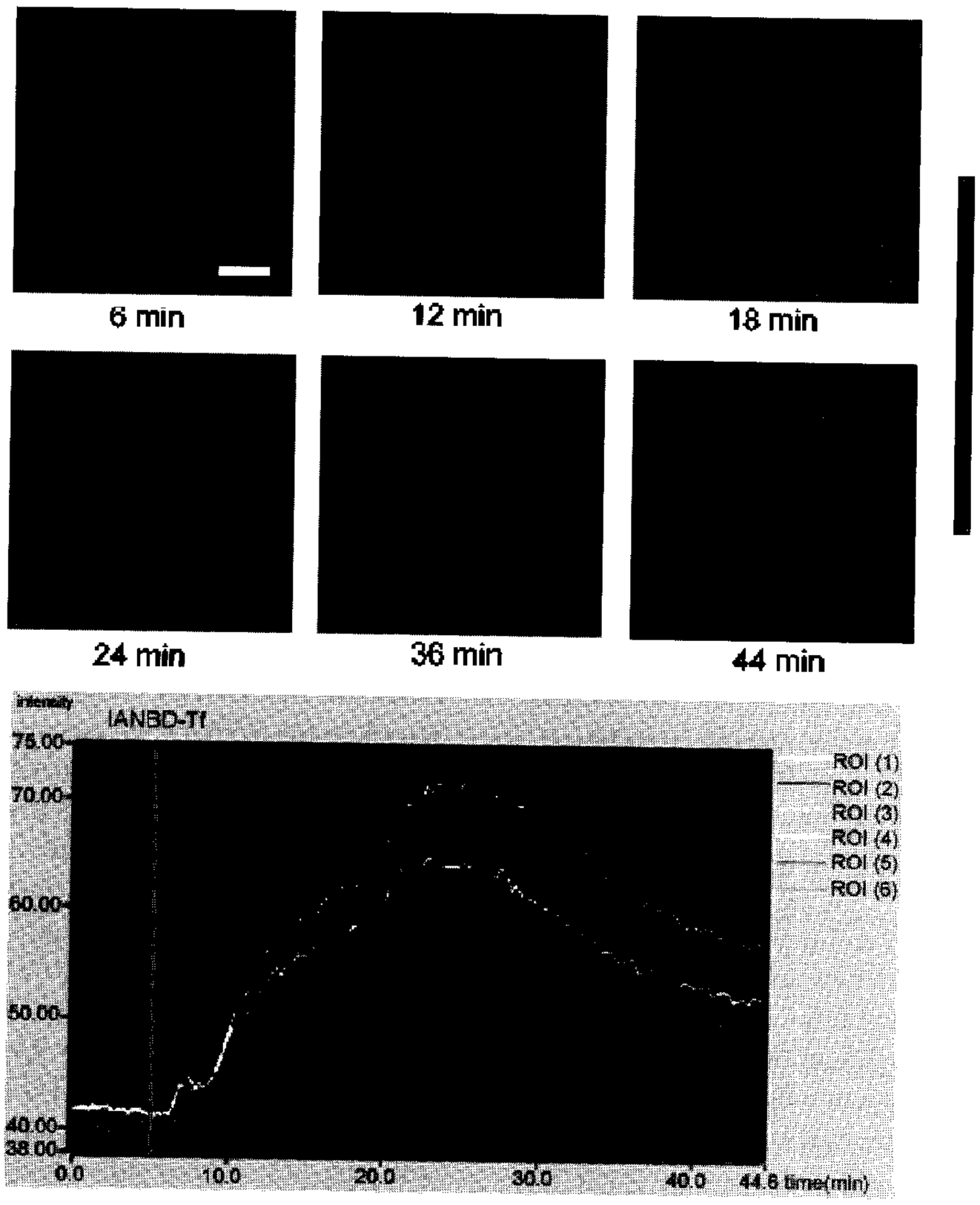

Fig. 4. The microscopic fluorescence images of the K562 cells at various indicated moments after addition of IANBD-labeled iron-saturated Tf. One milliliter cell suspension (5×10^5 cells/ml) was transferred to a glass-bottomed dish and incubated for 30 min at 37 °C. Then, the microscopic fluorescence images were taken every 20 s with exposure time of 500 ms for each image at excitation of 478 nm and emission above 515 nm. The cells were exposed to a pulsed IANBD–transferrin 6 min later after measurement started. The lower panel shows the kinetic changes of the fluorescence in six randomly selected cells. Magnification: 4×10^4; scale bar (on upper-left panel): 15 μm.

recycling was not affected by GF109203X in the cells that had not been activated by PMA. The results clearly indicate that the endocytosis and recycling of the Tf–TfR complex could be accelerated if PKC is activated. This result is consistent with the previous observation that the inhibitor of PKC can also reverse the acceleration of the Tf–TfR complex in $[Ca^{2+}]_i$-elevated cells (shown in Fig. 5C), since more PKC are translocated from cytosol to plasma membrane and activated by elevation of intracellular Ca^{2+}.

3.5. *Effect of intracellular Ca^{2+} and W-7 on the actin polymerization in cytoskeleton*

In order to find out whether the cytoskeleton plays a role in the regulation of iron uptake or the recycling of Tf–TfR complex by intracellular Ca^{2+}, actin polymerization in the cells preincubated with 2 and 5 nM TG was measured, respectively, and compared with that observed in the controlled cells and the cells preincubated with TG plus W-7. The results are shown in Fig. 7. It was found that the actin polymerization significantly increased when intracellular Ca^{2+} was raised by TG treatment. However, W-7 effectively reversed the enhancement of the polymerization by elevation

Table 1
The effects of thapsigargin and W-7 on the actin polymerization of cytoskeleton in K562 cells

Treatment of cells	Mean fluorescence due to F-actins per cell (arbitrary unit)
Control	11.5 ± 1.3
2 nM TG	14.1 ± 1.1
5 nM TG	16.4 ± 1.3
5 nM TG + 50 μM W-7	13.2 ± 0.4

Actin polymerization is shown as the mean fluorescence of the special F-actin probe BODIPY phallacidin per cell. Each data is the mean of three independent analyses of 10^4 cells.

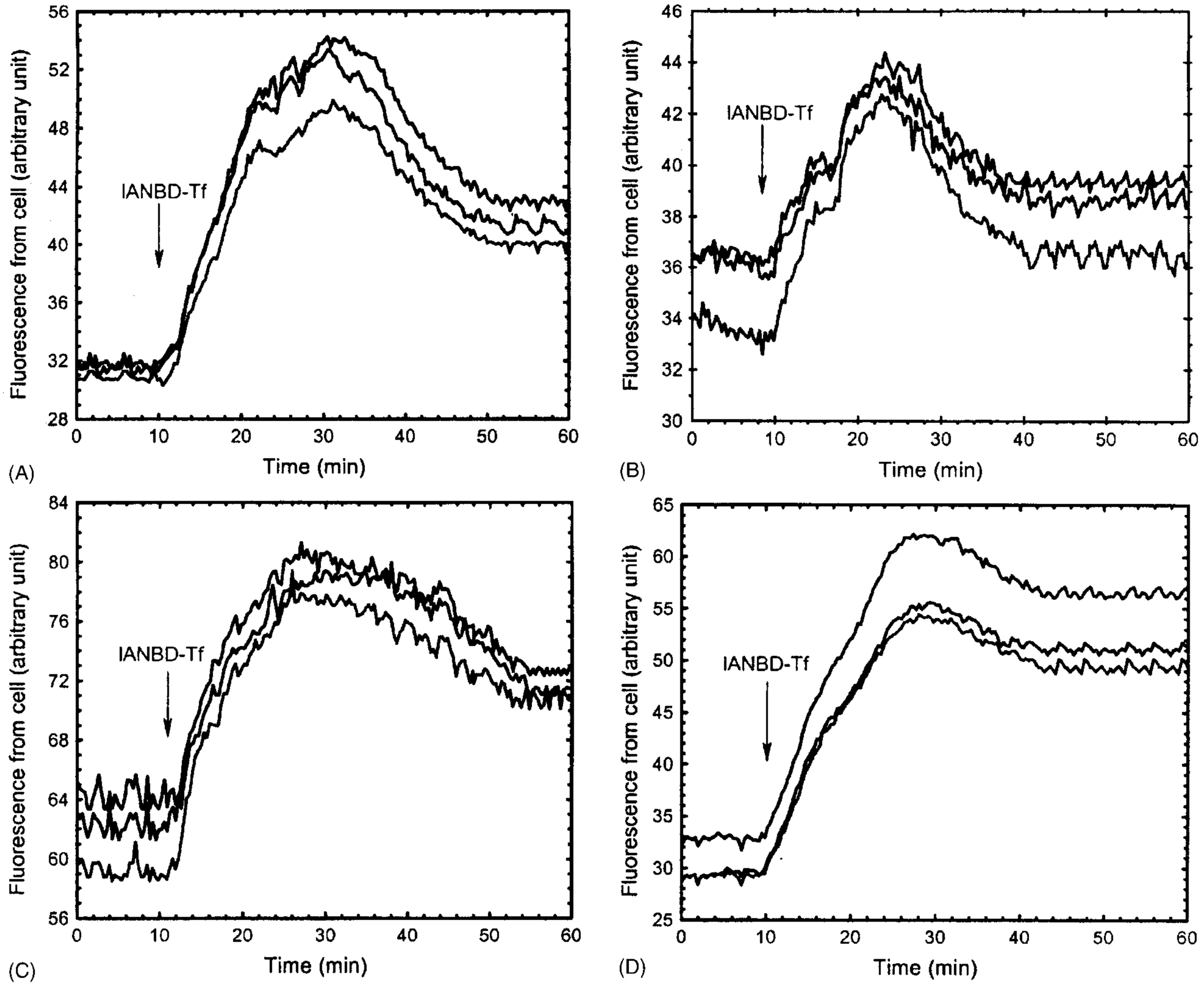

Fig. 5. The single-round kinetics of uptake and recycling of the IANBD-labeled transferrin in the K562 cells preincubated with thapsigargin, thapsigargin plus either GF109203X or W-7. Each dish contained 1 ml cell suspension (5×10^5 cells/ml). The cells were exposed to a pulsed IANBD-labeled transferrin 5 min later after the addition of thapsigargin. The fluorescence images of the cells attached to glass-bottomed dishes were taken every 20 s. The kinetics of the fluorescence from three randomly selected cells (excitation, 478 nm; emission, >520 nm) in controlled cells (A), the cells preincubated with 5 nM thapsigargin (B), the cells preincubated with 1 μM GF109203X for 25 min first and then 5 nM thapsigargin for additional 5 min (C), and the cells preincubated with 50 μM W-7 for 5 min first and then 5 nM thapsigargin for additional 5 min (D) were obtained from processing the corresponding images, respectively.

of $[Ca^{2+}]_i$. The quantitative parameters of actin polymerization measured as the mean fluorescence of the special F-actin probe BODIPY phallacidin per cell under the four different conditions are shown in Table 1. It seems that the actin polymerization in cytoskeleton is quite sensitive to the intracellular Ca^{2+} and calmodulin may play an important role in the intracellular Ca^{2+}-regulated actin polymerization.

4. Discussion

Release of iron from Tf in an acidic milieu of endosomes and its translocation into cytosol are integral steps in the process of iron uptake via TfR-mediated endocytosis. However, in almost all previous investigations, the TfR-mediated iron uptake was studied as the recycling of the receptor using either ^{125}I-labeled [14] or prebound biotinylated Tf (in tTA-HeLa cells) [29]. The observed recycling does not properly account for the release of iron from Tf in endosomes and its translocation into cytoplasmic pool in cells. In some other studies, although the iron uptake by cells was directly measured using radioisotope ^{59}Fe-bound or ^{55}Fe-bound Tf [30], the information obtained only concerned the quantity of the iron taken up by cells in a certain period of time. Besides that, the measured uptaken ^{59}Fe or ^{55}Fe are mainly associated with ferritin and other final targets. It does not properly reflect the initial steps of the iron uptake, namely the endocytosis of Tf and release of iron ions from Tf into cytosol. In the present study, because the non-invasive fluorescence detection and microscopic imaging of living cells

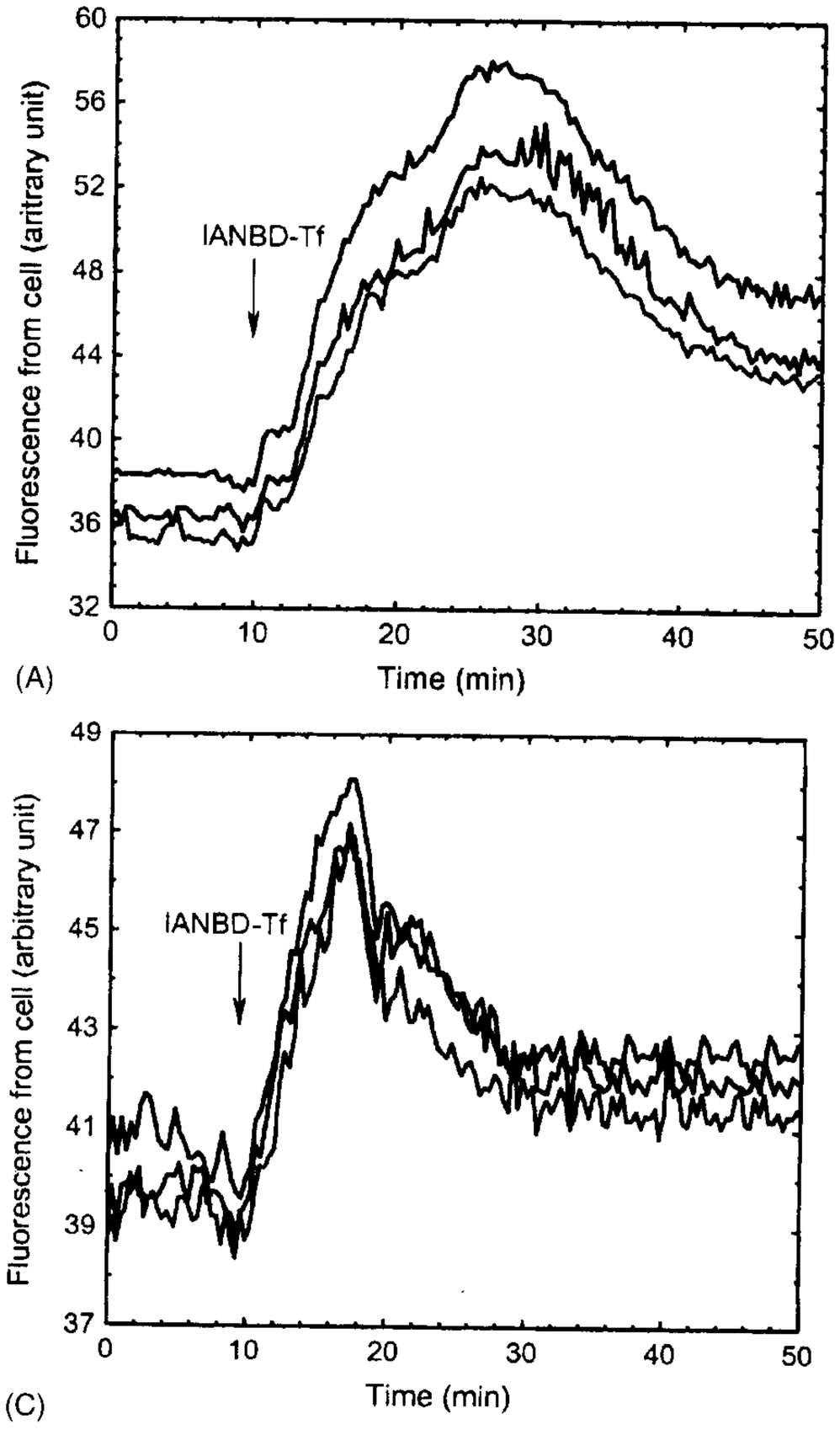

Fig. 6. The single-round kinetics of uptake and recycling of the IANBD-labeled transferrin in the K562 cells preincubated with PMA of different concentration and GF109203X. Each dish contained 1 ml cell suspension (5×10^5 cells/ml). The cells were exposed to a pulsed IANBD-labeled transferrin 10 min later after addition of PMA or 30 min later after addition of GF109203X. The fluorescence images of the cells attached to glass-bottom dishes were taken every 20 s. The kinetics of the fluorescence from three randomly selected cells (excitation, 478 nm; emission, >520 nm) in controlled cells (A), the cells preincubated with 10 nM PMA (B), or 100 nM PMA (C), and the cells preincubated with 1 μM GF109203X for 30 min (D) were obtained from processing the corresponding images, respectively.

were applied, disturbance from any pretreatment of biological samples is minimized. Not only the kinetic process of iron uptake in suspended cell population or in single living cells can be chased directly, the rate of iron uptake initiated by the binding of Tf to TfR can be precisely determined.

The present study shows that the intracellular free calcium, $[Ca^{2+}]_i$, plays an important role in regulating the TfR-mediated iron uptake in K562 cells. Elevation of $[Ca^{2+}]_i$ by preincubating cells with TG, a potent endomembrane Ca^{2+}-ATPase inhibitor which can release Ca^{2+} from intracellular store, speeds up the uptake and increases the overall capacity of the cells in taking up iron. In this study, BAPTA-AM was used to chelate intracellular Ca^{2+}. Does BAPTA also chelate the ferrous or ferric ions released from the entered Tf in the chelatable pool and prevent the fluorescence of calcein from quenching by iron? The answer seems negative. Although the affinity of BAPTA for the metals was $Fe^{3+} > Ca^{2+} > Fe^{2+}$ (the dissociation constants, K_d, of BAPTA for Ca^{2+}, Fe^{3+}, and Fe^{2+} are 1.1×10^{-7}, 5×10^{-9}, and 1×10^{-6} M, respectively) [31], the affinity constants of calcein for Fe^{2+} and Fe^{3+} (10^{14} and 10^{24} M^{-1}, respectively) [18] are much higher than the affinity constant of BAPTA for them. Therefore, the presence of BAPTA in cells would not affect the binding of iron ions to the fluorescence probe calcein. The fact that depletion of intracellular Ca^{2+} by BAPTA or complete chelation of extracellular Ca^{2+} by EGTA to stop Ca^{2+}-influx resulted in almost complete inhibition of the iron uptake give a further evidence of a strong calcium dependence in the TfR-mediated iron uptake. The ability of cells in taking up Tf-bound iron may be related to the number of TfRs on cell surface or to the capability of the cells in endocytosing the Tf–TfR complex.

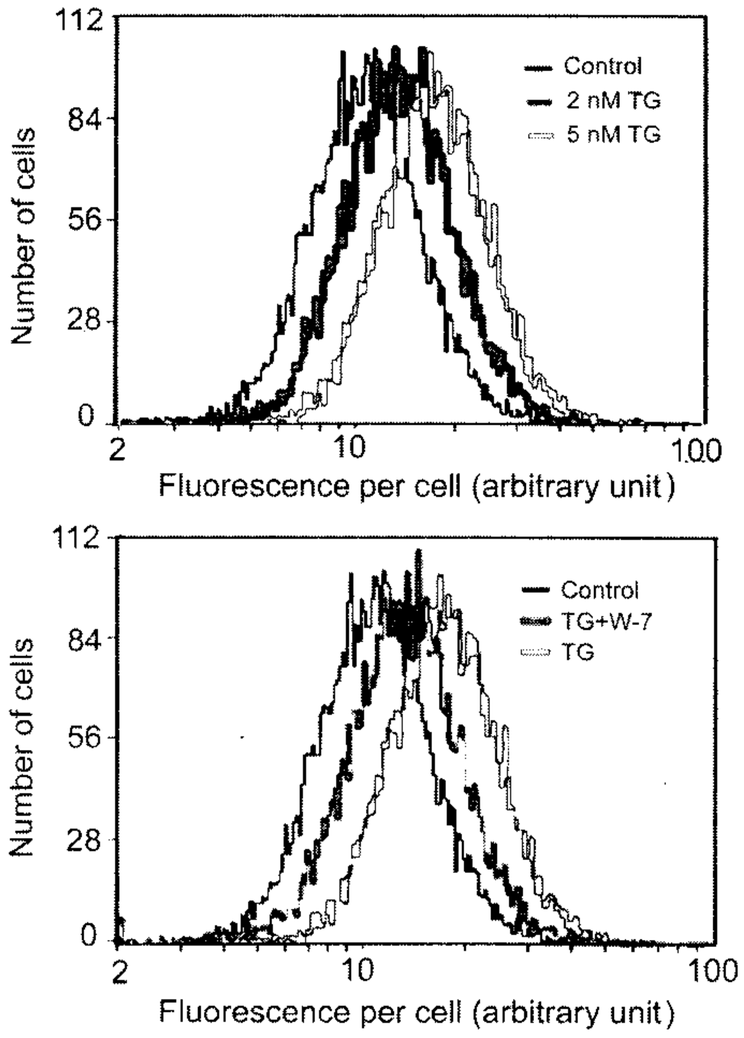

Fig. 7. Flow cytometric analysis of actin polymerization in K562 cells treated with thapsigargin or thapsigargin plus W-7. Cells (1×10^6/ml, 1 ml) were loaded with BODIPY FL phallacidin (1.5 units), and 10^4 cells in each sample were analyzed. The distributions of cell number against the fluorescence per cell in controlled cells, the cells preincubated with 2 and 5 nM thapsigargin, and the cells preincubated with 5 nM thapsigargin plus 20 μM W-7 are shown in different color and indicated with short legends.

The present study does show an increase of the TfRs expressed on cell surface in $[Ca^{2+}]_i$-elevated cells. However, the increase is not significant enough to account for the up-regulation of the cellular iron uptake. Therefore, more effort was made to investigate the effect of intracellular calcium on TfR-mediated endocytosis of the Tf–TfR complex.

In the present study, the single-round kinetics of uptake and recycling of the IANBD-labeled Tf visualized by consecutive fluorescence imaging of cells shows that elevation of cytosolic free Ca^{2+} accelerates not only outward flow but also the internalization of the Tf–TfR complex (see Fig. 5A and B). However, GF109203X, the selected cell-permeant inhibitor of PKC, and W-7, the calmodulin antagonist, can abolish such acceleration in $[Ca^{2+}]_i$-elevated cells (see Fig. 5C and D). These observations revealed that PKC and calmodulin might play some critical role in accelerating the recycling of the Tf–TfR complex.

It has been well established that calmodulin or some other Ca^{2+}-dependent proteins are activated when intracellular Ca^{2+} is elevated. The fact that inactivation of calmodulin by W-7 resulted in an abortion of acceleration of the Tf–TfR complex recycling clearly indicates that the activation of calmodulin or some other calcium-dependent proteins, such as some actin-binding proteins, may be one of the molecular mechanisms in accelerating endocytosis and recycling of the Tf–TfR complex. The actin cytoskeleton has been implicated in endocytic processes, but its necessity and roles in endocytosis remain ambiguous [32,33]. Most of the evidence suggesting a role of actin in endocytosis came from the studies in budding yeast. It was found that disruption of genes encoding actin and many actin-binding proteins block the uptake of endocytic markers [34]. Since actin polymerization into linear microfilaments may provide the force for pulling the endocytic vesicles from the cell surface and driving membrane fission or vesicles to move through the cytoplasm, it is reasonable to study the relationship between intracellular Ca^{2+} and the actin polymerization in cytoskeleton. In this study, it was found that the actin polymerization in TG-treated K562 cells increased markedly with increasing concentration of TG, the calcium-releasing agent (see the upper panel in Fig. 7). The degree of actin polymerization in 5 nM TG-treated cells is 40% higher than that in controlled cells (see Table 1). When 50 μM W-7, the calmodulin antagonist, is used, the actin polymerization in 5 nM TG-treated cells was reduced to the level slightly higher than that in controlled cells (see the lower panel in Fig. 7 and Table 1), and the corresponding endocytosis and recycling of Tf–TfR significantly slowed down (comparing Fig. 5D with B). These results suggest that the intracellular free calcium may regulate the TfR-mediated iron uptake through alteration of the actin polymerization in cytoskeleton, and calmodulin or some other Ca^{2+}-dependent actin-binding proteins may play an essential role in regulating actin cytoskeleton.

It has been also well established that elevation of intracellular Ca^{2+} level promotes translocation of PKC from cytosol to plasma membrane and facilitates their activation. When PKC inhibitor GF109203X is present, abortion of the accelerated endocytosis, and recycling of Tf–TfR complex in $[Ca^{2+}]_i$-elevated cells might imply the involvement of PKC activation in the intracellular Ca^{2+}-induced acceleration of the endocytosis and recycling. In order to further investigate the role of PKC, PMA, the direct activator of PKC, was used to prime cells and see whether it can speed up the endocytosis or recycling of the complex. As shown in Fig. 6, a positive result was observed. The higher the concentration of PMA, the shorter the time needed for completing the transcytosis. The reverse effect of GF109203X on the recycling of Tf–TfR complex in $[Ca^{2+}]_i$-elevated cells together with the priming effect of PMA on the recycling of Tf–TfR complex in controlled cells suggest that the translocation and activation of PKC is the other molecular mechanism involved in speeding up the endocytosis and recycling of the Tf–TfR complex by intracellular Ca^{2+}. Increasing evidence has illustrated that PKC is capable of translocation to other subcellular sites, including other membrane vesicles and cytoskeleton besides plasma membrane, upon activation by calcium [35]. The activated PKC may lead actin rearrangement by phosphorylating a wide range of cytoskeletal components [36,37]. It was reported that PMA accelerated growth of F-actin in isolated bipolar cells [38]. This study suggests that some activated isoforms of PKC may regulate the actin cytoskeleton and then speed up the transcytosis of the complex when intracellular Ca^{2+} is raised.

Acknowledgements

This work was supported by the National Natural Science Foundation of China (No. 39670205), Hong Kong UGC Grant (BQ-445), and The Hong Kong Polytechnic University Research Grants (A-PC23). We are indebted to Hamamatsu Photonics K.K. for providing us Microscopic Image Acquisition and Analysis System.

References

[1] H.M. Lederman, A. Cohen, J.W. Lee, M.H. Freedman, E.W. Gelfand, Desferoxamine: a reversible S-phase inhibitor of human lymphocyte proliferation, Blood 64 (1980) 748–753.
[2] L.C. Kühn, H.M. Schulman, P. Ponka, Iron-transferrin requirements and transferrin receptor expression in proliferating cell, in: Iron Transport and Storage, CRC Press, Boca Raton, FL, 1990, pp. 149–191.
[3] P. Galan, S. Hercberg, Y. Touitou, The activity of tissue enzymes in iron-deficient rat and man: an overview, Comp. Biochem. Physiol. B 77 (1984) 647–653.
[4] B. Halliwell, J.M.C. Gutteridge, Role of free radicals and catalytic metal ions in human diseases: an overview, Methods Enzymol. 186 (1990) 1–85.
[5] P. Aisen, M. Wessling-Resnick, E.A. Leibold, Iron metabolism, Curr. Opin. Chem. Biol. 3 (1999) 200–206.
[6] K.A. Jellinger, The role of iron in neurodegeneration, Drugs Aging 14 (1999) 115–140.
[7] Z.M. Qian, Q. Wang, Expression of iron transport proteins and excessive iron accumulation of iron in the brain in neurodegenerative disorders, Brain Res. Rev. 27 (1998) 257–267.
[8] K.F. Swaiman, Hallervorden-Spatz and brain iron metabolism, Arch. Neurol. 48 (1991) 1285–1293.
[9] D.M.D. Silva, C. Askwith, J. Kaplan, Molecular mechanisms of iron uptake in eukaryotes, Physiol. Rev. 76 (1996) 31–47.
[10] Z.M. Qian, P.L. Tang, Mechanism of iron uptake by mammalian cells, Biochim. Biophys. Acta 1269 (1995) 205–214.
[11] G. Weiss, T. Houston, S. Kastner, K. Johrer, K. Grunewald, J.H. Brock, Regulation of cellular iron metabolism by erythropoietin: activation of iron-regulatory protein and up regulation of transferrin receptor expression in erythroid cells, Blood 89 (1997) 680–687.
[12] B. Guo, F.M. Brown, J.D. Phillips, Y. Yu, E.A. Leibold, Characterization and expression of iron regulatory protein 2 (IRP2). Presence of multiple IRP2 transcripts regulated by intracellular iron levels, J. Biol. Chem. 270 (1995) 16529–16535.
[13] A.M. Thomson, J.T. Rogers, P.J. Leedman, Thyrotropin-releasing hormone and epidermal growth factor regulate iron-regulatory protein binding in pituitary cells via protein kinase C-dependent and-independent signaling pathways, J. Biol. Chem. 275 (2000) 31609–31615.
[14] J. Sainte-Marie, V. Lafont, E.I. Pecheur, J. Favero, J.R. Philippot, A. Bienvenue, Transferrin receptor functions as a signal-transduction molecule for its own recycling via increases in the internal Ca^{2+} concentration, Eur. J. Biochem. 250 (1997) 689–697.
[15] R.R. Crichton, R.J. Ward, Iron metabolism—new perspectives in view, Biochemistry 31 (1992) 11255–11264.
[16] S. Pollack, Receptor-mediated iron uptake and intracellular iron transport, Am. J. Hematol. 39 (1992) 113–118.
[17] R.J. Rothman, A. Serroni, J.H. Farer, Cellular pool of transient ferric iron, chelatable by desferoxamine and distinct from ferritin, Mol. Pharmacol. 42 (1992) 703–710.
[18] W. Breuer, S. Epsztezn, Z.I. Cabantchik, Iron acquired from transferrin by k562 cells is delivered into a cytoplasmic pool of chelatable iron(II), J. Biol. Chem. 70 (1995) 24209–24215.
[19] O. Thastrup, B. Foder, O. Scharff, The calcium mobilizing and tumor-promoting agent, thapsigargin elevates the platelet cytoplasmic free calcium concentration to a higher steady state level. A possible mechanism of action for the tumor promotion, Biochem. Biophys. Res. Commun. 142 (1987) 654–660.
[20] O. Thastrup, P.J. Cullen, B.K. Drobak, M.R. Hanley, A.P. Dawson, Thapsigargin, a tumor promoter, discharges intracellular Ca^{2+} stores by specific inhibition of the endoplasmic reticulium Ca^{2+} ATPase, Proc. Natl. Acad. Sci. U.S.A. 87 (1990) 2466–2470.
[21] J.D. Shore, D.E. Day, A.M. Francis-Chmura, I. Verhamme, J. Kvassman, D.A. Lawrence, D. Ginsburg, A fluorescent probe study of plasminogen activator inhibitor-1: evidence for reactive center loop insertion and its role in the inhibitory mechanism, J. Biol. Chem. 270 (1995) 5395–5398.
[22] R.Y. Tsien, T.J. Rink, M. Poenie, Measurement of cytosolic free Ca^{2+} in individual small cells using fluorescence microscopy with dual excitation wavelengths, Cell Calcium 6 (1985) 145–157.
[23] M.U. Ehrengruber, T.D. Coates, D.A. Deranleau, Shape oscillations: a fundamental response of human neutrophils stimulated by chemotactic peptides? FEBS Lett. 359 (1995) 229–232.
[24] H. Hidaka, T. Yamaki, M. Naka, T. Tanaka, H. Hayashi, R. Kobayashi, Calcium-regulated modulator protein interacting agents inhibit smooth muscle calcium-stimulated protein kinase and ATPase, Mol. Pharmacol. 17 (1980) 66–72.
[25] K. Takahashi, K. Tago, H. Okano, Y. Ohya, T. Katada, Y. Kanaho, Augmentation by calmodulin of ADP ribosylation factor-stimulated phospholipase D activity in permeabilized rabbit peritoneal neutrophils, J. Immunol. 156 (1996) 1229–1234.
[26] E. Capuozzo, D. Verginelli, C. Crifo, C. Salerno, Effects of calmodulin antagonists on calcium pump and cytosolic calcium level in human neutrophils, Biochim. Biophys. Acta 1357 (1997) 124–127.
[27] I. Hers, J.M. Tavare, R.M. Denton, The protein kinase C inhibitors bisindolylmaleimide I (GF 109203x) and IX (Ro 31-8220) are potent inhibitors of glycogen synthase kinase-3 activity, FEBS Lett. 460 (1999) 433–436.
[28] J.A. Rosado, A. Gonzalez, G.M. Salido, J.A. Pariente, Effects of reactive oxygen species on actin filament polymerization and amylase secretion in mouse pancreatic acinar cells, Cell Signal. 14 (2002) 547–556.
[29] B.P. Ceresa, M. Lotscher, S.L. Schmid, Receptor and membrane recycling can occur with unaltered efficiency despite dramatic Rab5 (Q79L)-induced changes in endosome geometry, J. Biol. Chem. 276 (2001) 9649–9654.
[30] D.R. Richardson, The role of the membrane-bound tumor antigen, melanotransferrin (p97), in iron uptake by the human malignant melanoma cell, Eur. J. Biochem. 267 (2000) 1290–1298.
[31] B.E. Britigan, G.T. Rasmussen, C.D. Cox, Binding of iron and inhibition of iron-dependent oxidative cell injury by the calcium chelator 1,2-bis(2-aminophenoxy) ethane *N,N,N′,N′*-tetraacitic acid (BAPTA), Biochem. Pharmacol. 55 (1998) 287–295.
[32] R.L. Jeng, M.D. Welch, Cytoskeleton: actin and endocytosis—no longer the weakest link, Curr. Biol. 11 (2001) R691–R694.
[33] B. Qualmann, M.M. Kessel, R.B. Kelly, Molecular links between endocytosis and actin cytoskeleton, J. Cell Biol. 150 (2000) F111–F116.
[34] A.L. Munn, Molecular requirements for the internalization step of endocytosis: insights from yeast, Biochim. Biophys. Acta 1535 (2001) 236–257.
[35] C. Keenan, D. Kelleher, Protein kinase C and the cytoskeleton, Cell Signal. 10 (1998) 225–232.
[36] M.V. Parsey, G.K. Lewis, Actin polymerization and pseudopod reorganization accompany anti-CD3-induced growth arrest in Jurkat T cells, J. Immunol. 151 (1993) 1881–1893.
[37] G.P. Downey, C.K. Chan, P. Lea, A. Takai, S. Grinstein, Phorbol ester-induced actin assembly in neutrophils: role of protein kinase C, J. Cell Biol. 116 (1992) 695–706.
[38] C. Job, L. Lagnado, Calcium and protein kinase regulate the actin cytoskeleton in the synaptic terminal of retinal bipolar cells, J. Cell Biol. 143 (1998) 1661–1672.